Surface Densities Prewet a Near Critical Membrane
Supplementary Material

Mason Rouches, Sarah L. Veatch, Benjamin B. Machta

Contents

Overview

In section 1 we provide details on the Landau Theory introduced in the main text. We first derive the Landau coefficients used in our expression of the tether free energy, f_{tether}. Next we detail the derivation of the surface free energy, f_{surf} expressed as a function of three 'surface' variables ϕ_0,ψ,ρ. We then examine the behavior of f_{surf} near the membrane critical point, showing enhancement of prewetting through the diverging effective surface enhancement and surface chemical potential as criticality is approached. We then derive a relationship between membrane's susceptibility and the enhancement of prewetting. In Section 2 we provide the supplemental figures referenced in the main text. Here we discuss the effect of finite tether-length used in our simulations, properties of our bulk lattice polymers system and alternative polymer mixtures, expand on the three-phase coexistence region, and discuss membrane- and bulk-dominated surface denstites

1 Landau Theory

Our mean-field theory starts with the Landau Functional shown in Equation 1 of the main text:

$$\begin{aligned}
\mathcal{L} &= \mathcal{L}_{2D} + \mathcal{L}_{3D} \\
\mathcal{L}_{2D} &= \int d^2\vec{x} f_{2D}(\psi, \rho, \phi_0) \\
\mathcal{L}_{3D} &= \int d^2\vec{x} dz \frac{1}{2}\nabla\phi^2 + f_{3D}(\phi) \\
f_{2D}(\psi, \rho, \phi_0) &= \underbrace{\frac{t_{mem}}{2}\psi^2 + \frac{u_{mem}}{4!}\psi^4 - \lambda_\psi\psi}_{f_{membrane}} \\
&\quad \underbrace{- \frac{5}{6}\rho + \frac{3}{2}\rho^2 - \frac{3}{3!}\rho^3 + \frac{2}{4!}\rho^4 - \frac{1}{4} - \lambda_\rho\rho}_{f_{tether}} \\
&\quad \underbrace{- h_\psi\rho\psi - h_\phi\rho\phi_0}_{f_{int}}
\end{aligned} \tag{1}$$

where f_{3D} is the free energy of a system displaying a conventional condensation transition:

$$f_{3D} = \frac{t_{bulk}}{2}\phi^2 + \frac{u_{bulk}}{4!}\phi^4 - \mu_{bulk}\phi \tag{2}$$

Our goal is to minimize $\mathcal{L}$ over order parameters ρ,ψ and order parameter profile $\phi(z)$. Two derivatives $\frac{\partial\mathcal{L}}{\partial\psi} = \frac{\partial\mathcal{L}}{\partial\rho} = 0$ minimize the free energy over purely 'surface' terms. A functional derivative $\frac{\delta\mathcal{L}}{\delta\phi(z)} = 0$ minimizes the energy over forms of the density profile $\phi(z)$.

1.1 Derivation of f_{tether}

The free energy of the tethers in our model is expressed as a Landau free energy, a function of powers of the order parameter ρ and Landau coefficients a,b,c,d,e

$$f_{tether}(\rho) = a\rho + \frac{b}{2}\rho^2 + \frac{c}{3!}\rho^3 + \frac{d}{4!}\rho^4 + e - \lambda_\rho\rho$$

The tethers are a non-interacting 2-dimensional lattice gas. The free energy of a 2D gas may be written as $f_{tether} = \rho\log\rho$. We approximate this by expanding f_{tether} in powers of ρ at $\rho_\star$

$$\rho\log\rho|_{\rho_\star} = (\rho - \rho_\star)(1 + \log\rho_\star) + \frac{(\rho-\rho_\star)^2}{2\rho_\star} - \frac{(\rho-\rho_\star)^3}{6\rho_\star^2} + \frac{(\rho-\rho_\star)^4}{12\rho_\star^3}$$

$$f_{tether}(\rho, \rho_\star) = \frac{-3\rho_\star^4 - 12\rho_\star^4\log\rho_\star}{12\rho_\star^3} + \frac{\rho\left(-10\rho_\star^3 + 12\rho_\star^3\log\rho_\star\right)}{12\rho_\star^3} + \frac{3\rho^2}{2\rho_\star} - \frac{\rho^3}{2\rho_\star^2} + \frac{\rho^4}{12\rho_\star^3} - \lambda_\rho\rho$$

Setting $\rho_\star = 1$, as used in all calculations here, we obtain the free energy of the tethers and values of all Landau coefficients:

$$f_{tether}(\rho, \rho_\star = 1) = -\frac{1}{4} - \frac{5}{6}\rho + \frac{3}{2}\rho^2 - \frac{3}{3!}\rho^3 + \frac{2}{4!}\rho^4 - \lambda_\rho\rho$$

This Taylor series provides an analytically tractable approximation to the ideal gas free energy of the tethers near $\rho = 1$. However, because its first derivative is finite at $\rho = 0$, some of our physical phases spill over into negative values of ρ. As such we interpret ρ more as an order parameter than as a more rigorously defined tether density.

1.2 Derivation of surface free-energy

Contributions from the bulk are a function of $\phi(z)$. To simplify calculations we express the bulk energy as a function of initial and final values of ϕ, $\phi(z=0)=\phi_0$ and $\phi(z=\infty)=\phi_\infty$. these solely determine the behaviour of the density profile. We write $f_{3D}(\phi)-f_{3D}(\phi_\infty)$ as $f_{3D}^{\phi-\phi_\infty}$.

First we perform the functional derivative, $\frac{\delta\mathcal{L}_{bulk}}{\delta\phi(z)}$

$$\begin{aligned}
\mathcal{L}_{bulk}(\phi(z)) &= \int_0^\infty dz \frac{1}{2}(\nabla\phi)^2 + f_{3D}^{\phi-\phi_\infty} \\
\delta\mathcal{L}_{bulk}[\phi(z)] &= \int_0^\infty dz \nabla\phi\nabla\delta\phi + \frac{\partial f_{3D}^{\phi-\phi_\infty}}{\partial\phi}\delta\phi \\
\frac{\delta\mathcal{L}_{bulk}[\phi(z)]}{\delta\phi(z)} &= \frac{\partial f_{3D}^{\phi-\phi_\infty}}{\partial\phi} - \nabla^2\phi = 0
\end{aligned} \tag{3}$$

The last equality serves as a second order ODE for $\phi(z)$ which we solve given boundary conditions at $z=0,\infty$, making use of mathematical tools developed in [1].

$$\begin{aligned}
\frac{\delta\mathcal{L}_{bulk}}{\delta\phi(z)} &= 0 \\
\frac{\partial^2\phi}{\partial z^2} &= \frac{\partial f_{3D}^{\phi-\phi_\infty}}{\partial\phi} \\
\frac{\partial\phi}{\partial z}\frac{\partial^2\phi}{\partial z^2} &= \frac{\partial\phi}{\partial z}\frac{\partial f_{3D}^{\phi-\phi_\infty}}{\partial\phi} \\
\frac{1}{2}\frac{\partial}{\partial z}\left(\frac{\partial\phi}{\partial z}\right)^2 &= \frac{\partial}{\partial z}f_{3D}^{\phi-\phi_\infty} \\
\frac{1}{2}\int_{z=0}^{z=\infty} dz\frac{\partial}{\partial z}\left(\frac{\partial\phi}{\partial z}\right)^2 &= \int_{z=0}^{z=\infty} dz f_{3D}^{\phi-\phi_\infty} \\
\frac{1}{2}\left(\left(\frac{\partial\phi}{\partial z}\right)^2_{z=\infty} - \left(\frac{\partial\phi}{\partial z}\right)^2_{z=0}\right) &= f_{3D}^{\phi-\phi_\infty}(\phi_\infty) - f_{3D}^{\phi-\phi_\infty}(\phi_0) \\
\frac{1}{2}\left(\frac{\partial\phi}{\partial z}\right)^2_{z=0} &= f_{3D}^{\phi-\phi_\infty}(\phi_0) \\
\frac{\partial\phi}{\partial z} &= \pm\sqrt{2f_{3D}^{\phi-\phi_\infty}(\phi_0)}
\end{aligned} \tag{4}$$

Finally we substitute this into our original functional and rewrite as an integration over values

of ϕ instead of z to define the bulk contribution, Δf_{bulk}

$$\begin{aligned}
\Delta f_{bulk}(\phi(z)) &= \int_0^\infty dz \frac{1}{2} (\nabla\phi)^2 + f_{3D}^{\phi-\phi_\infty} \\
&= \int_0^\infty dz \, (\nabla\phi)^2 \\
&= \int_{\phi_0}^{\phi_\infty} dz \frac{d\phi}{dz}\frac{dz}{d\phi} (\nabla\phi)^2 \\
&= \int_{\phi_0}^{\phi_\infty} d\phi \nabla\phi \\
\Delta f_{bulk}(\phi_0, \phi_\infty) &= \int_{\phi_0}^{\phi_\infty} d\phi \sqrt{(2(f_{\phi_0} - f_{\phi_\infty}))}
\end{aligned} \tag{5}$$

The sign of $\frac{\partial\phi}{\partial z}$ depends on whether ϕ_0 is above or below ϕ_∞: polymer density always moves towards the bulk density ϕ_∞. An expression for the gradient may be obtained by substituting in the expression for $f_{3D}^{\phi-\phi_\infty}(\phi)$ and $u_{bulk} = \frac{1}{6}\left(6t_{bulk}\phi_\infty + \phi_\infty^3\right)$:

$$\frac{\partial\phi}{\partial z} = (\phi - \phi_\infty)\frac{\sqrt{(12t_{bulk} + \phi^2 + 2\phi\phi_\infty + 3\phi_\infty^2)}}{2\sqrt{6}} \tag{6}$$

Writing Δf_{bulk} as a function of ϕ_0 and ϕ_∞ now allows minimization of the systems Landau free energy over values of ϕ_0,ρ, and ψ. After solutions are obtained we compute the energy of each of these solutions. This can be expressed as

$$\begin{aligned}
f_{surf} &= \Delta f_{bulk}(\phi_0, \phi_\infty) + f_{2D}(\phi_0, \psi, \rho) \\
&= \int_{\phi_0}^{\phi_\infty} d\phi \sqrt{2(f_{\phi_0} - f_{\phi_\infty})} + f_{2D} \\
f_{surf} &= \int_{\phi_0}^{\phi_\infty} d\phi \left\{ \nabla\phi - \frac{\partial f_{2D}}{\partial\phi} \right\} + \frac{\partial f_{2D}}{\partial\phi}|_{\phi_\infty}
\end{aligned} \tag{7}$$

where the final equation is the is the integration between the curves of $\nabla\phi$ and $-\frac{\partial f_{2D}}{\partial\phi_0}$ shown in Figure 5B of the main text.

1.3 Enhancement of prewetting regime near membrane critical point

In our Monte-Carlo simulations and numerical calculations, we find a large expansion of the prewetting region as the membrane is brought near to its critical point. We now aim to show using a simplified Landau theory how this enhancement arises. First we simplify the free energies of membrane and tether components, and obtain expressions for minimal values of ψ and ρ to quadratic order:

$$f_{2D} = \frac{t_{mem}}{2}\psi^2 - \lambda_\psi\psi - \frac{1}{4} - \frac{5}{6}\rho + \frac{3}{2}\rho^2 - \lambda_\rho\rho - h_\psi\psi\rho - h_\phi\phi_0\rho$$

$$\frac{\partial f_{2D}}{\partial \psi} = \frac{\partial f_{2D}}{\partial \rho} = 0$$
$$\psi_{min} = -\frac{-5h_\psi - 6\left(h_\psi \lambda_\rho - 3\lambda_\psi - h_\phi h_\psi \phi_0\right)}{6\left(3t_{mem} - h_\psi^2\right)}$$
$$\rho_{min} = -\frac{5t_{mem} - 6\left(t_{mem}\lambda_\rho + h_\phi \lambda_\psi + t_{mem} h_\phi \phi_0\right)}{6\left(h_\psi^2 - 3t_{mem}\right)} \tag{8}$$

This simplification of f_{2D} excludes fourth order terms in ψ and ρ is only reasonable for $t_{mem} > t_{c,mem}$. Substituting ψ_{min},ρ_{min} into the original f_{surf} we obtain the surface free energy in terms of ϕ_0:

$$f_{surf}(\phi_0, \psi, \rho) = \Delta f_{bulk}(\phi_0, \phi_\infty) - \frac{t_{mem} h_\phi^2}{2(3t_{mem} - h_\psi^2)}\phi_0^2 - \frac{h_\phi\left(t_{mem}\left(5 + 6\lambda_\rho\right) + 6h_\psi \lambda_\psi\right)}{6(3t_{mem} - h_\psi^2)}\phi_0$$
$$- \frac{t_{mem}\left(79 + 60\lambda_\rho + 36\lambda_\rho^2\right) + 6\left(-3h_\psi^2 + 2h_\psi\left(5 + 6\lambda_\rho\right)\lambda_\psi + 18\lambda_\psi^2\right)}{72(3t_{mem} - h_\psi^2)} \tag{9}$$

Here second order couplings in ϕ_0 emerge after the minimizing over the membrane and tether degrees of freedom. Each of these terms has a denominator, $3t_{mem} - h_\psi^2$ which defines the membrane critical point as $t_{mem} = h_\psi^2/3$. The surface enhancement (prefactor to the ϕ_0^2 term) is proportional to $(J_{c,mem} - J_{mem})^{-1}$ which is consistent with the scaling of the Ising model susceptibility exponent $\gamma = 1$ in mean-field.

1.4 Membrane susceptibility and prewetting

The susceptibility-mediated enhancement of prewetting can be seen directly by examining higher-order interactions between membrane and tether components. We split $\mathcal{L}_{2D}$ into non-interacting membrane and tether contributions and interaction terms mixing all components:

$$\mathcal{L}_{2D} = \int d^2\vec{x}\{f_{mem}(\psi) + f_{tether}(\rho) + f_{int}(\psi, \rho, \phi_0)\}$$
$$f_{int}(\psi, \rho, \phi_0) = -h_\psi \rho\psi - h_\phi \rho\phi_0 \tag{10}$$

We focus on the interactions and define $\mathcal{L}_{int} = \int d^2\vec{x} f_{int}(\psi, \rho, \phi_0)$. We calculate $\mathcal{L}_{int}$ as a sum of cumulants:

$$\mathcal{L}_{int} \approx \mathcal{L}_{int}^0 - \langle\mathcal{L}_{int}\rangle - \frac{1}{2}\left(\langle\mathcal{L}_{int}^2\rangle - \langle\mathcal{L}_{int}\rangle^2\right) - \ldots$$
$$\langle\mathcal{L}_{int}\rangle = \int d^2\vec{x} h_\psi \psi\rho + h_\phi \phi_0 \rho$$
$$\langle\mathcal{L}_{int}^2\rangle = \int d^2\vec{x}\rho(h_\psi\psi + h_\phi\phi_0)\int d^2\vec{x'}\rho'(h_\psi\psi' + h_\phi\phi_0)$$
$$\langle\mathcal{L}_{int}\rangle^2 = \left(\int d^2\vec{x} h_\psi\psi\rho + h_\phi\phi_0\rho\right)^2 \tag{11}$$

We assume $t_{mem} > t_{c,mem}$ and the membrane is at it's critical composition, $\psi = 0$. We assume we are far from the prewetting critical point and neglect second order terms in ϕ_0

$$
\begin{aligned}
\langle \mathcal{L}_{int} \rangle &= \langle \rho \rangle (h_\phi \langle \phi_0 \rangle + h_\psi \langle \psi \rangle) \\
\left\langle \mathcal{L}_{int}^2 \right\rangle - \langle \mathcal{L}_{int} \rangle^2 &= h_\psi^2 \langle \rho \rangle^2 \int d^2\vec{x} \psi_x \int d^2\vec{x'} \psi_{x'} - \left(\int d^2\vec{x} h_\psi \psi_x \rho_x \right)^2 \\
&= h_\psi^2 \langle \rho \rangle^2 \int d^2\vec{x} \int d^2\vec{x'} \langle \psi_x \psi_{x-x'} \rangle - h_\psi^2 \langle \rho \rangle^2 \langle \psi_x \rangle^2 \\
&= h_\psi^2 \langle \rho \rangle^2 \int d^2\vec{x} \langle \psi_x^2 \rangle - \langle \psi_x \rangle^2 \\
&= h_\psi^2 \langle \rho \rangle^2 \int d^2\vec{x} G(\vec{x}) \\
&= h_\psi^2 \langle \rho \rangle^2 \int dr G(r) \\
&= h_\psi^2 \langle \rho \rangle^2 \chi_\psi
\end{aligned} \tag{12}
$$

Here χ_ψ is the susceptibility of the membrane and $G(r)$ is the two-point correlation function. The integral over all space of $G(r)$ is χ_ψ. Here we have assumed that the membrane order parameter is translationally invariant and that $G(r)$ is spherically symmetric.

$$
\mathcal{L}_{int} \approx \mathcal{L}_{int}^0 - \langle \rho \rangle \left(h_\phi \langle \phi_0 \rangle + h_\psi \langle \psi \rangle \right) - \frac{h_\psi^2 \langle \rho \rangle^2}{2} \chi_\psi \tag{13}
$$

At the critical composition, $\psi = 0$ and critical temperature, $\chi_\psi \to \infty$, implying that interactions become very favorable even with negligible contributions from other terms. Substituting $\mathcal{L}_{int}$ into our original Landau functional, we obtain a new free energy function, neglecting fourth order terms:

$$
f_{2D} = -\frac{5}{6}\rho + \frac{3}{2}\rho^2 - \frac{1}{4} - \lambda_\rho \rho - h_\phi \phi_0 \rho - \frac{h_\psi^2 \rho^2}{2} \chi_\psi \tag{14}
$$

Minimizing over ψ and ρ and substituting back in the free energy, as in equation 9 above, we express f_{2d} just in terms of surface polymer density ϕ_0

$$
f_{2D} = -\frac{h_\phi^2}{2(h_\psi^2 \chi_\psi - 3)} \phi_0^2 + \frac{h_\phi (5 + 6\lambda_\rho)}{6(h_\psi^2 \chi_\psi - 3)} \phi_0 + \frac{-18 h_\psi^2 \chi_\psi + 36\lambda_\rho^2 + 60\lambda_\rho + 79}{72(h_\psi^2 \chi_\psi - 3)} \tag{15}
$$

This is similar to Equation 9, where the denominator vanishes at the 'shifted' membrane critical point $\chi_\psi = \frac{3}{h_\psi^2}$. This differs from the calculation above where the divergence near the critical point is stronger, as the Ising susceptibility exponent $\gamma = 7/4$ instead of 1. A full treatment of our model beyond mean-field would likely expand prewetting boundaries beyond the values we present here.

2 Supplementary Figures

2.1 Effect of tether length in monte-carlo simulations

Our Monte Carlo Simulations implement tethers with a finite three-dimensional length while the tethers in our landau theory lack a three-dimensional component. We examined the effect of tether length with simulations varying tether length from $1 - 10$ mononmers S1. As expected, prewet phases are stable at higher bulk temperatures as tether length is increased. The form of the polymer density profile is influenced by tether length. The density profile has a maximum at short but non-zero distances from the wall (see Main text Figure 2D,Figure 3C, S1). The location of this maximum extends further from the wall as tether length is increased. This is in contrast to conventional wetting and prewetting where the density profile is monotonic with distance from the membrane.

The non-standard behavior of the density profile is explained by the entropic repulsion experienced by polymers near a surface. Along the length of the tether, the membrane- and tether-mediated interactions between polymers are the same. However there are more interactions available to polymers at finite distance from the surface. With a non-zero tether length, polymers prefer to concentrate their density away from the surface while still within the tether length.

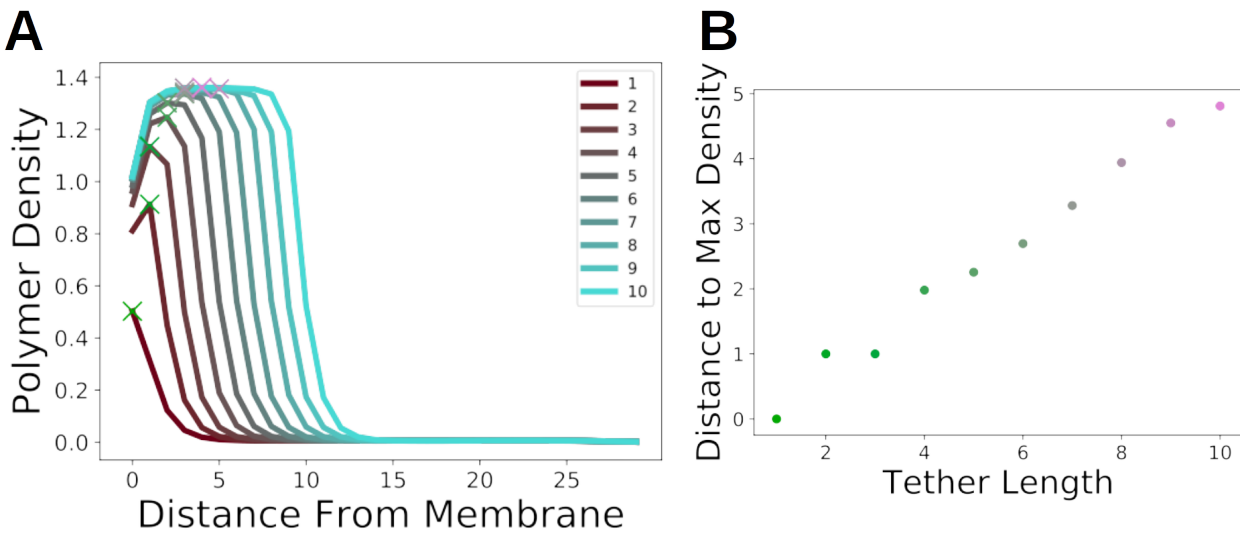

Figure S1: **Effect of Tether Length A**) Density profiles of simulations at various tether lengths. Simulations with longer tethers have a broader maximum further from the membrane. **B**) Distance of maximum polymer Density plotted against tether length

2.2 Simulations of bulk polymer mixtures

Our 3D lattice polymer simulations phase-separate into coexisting dense and dilute phases in-lieu of membrane and tethers. Here, as in the main text, red and blue polymers of equal length (n=20 monomer units) interact attractively with one another and like polymers repel each other. Polymers phase-separate through increasing J_{bulk} (See Figure S2). Higher polymer concentrations phase-separate at lower J_{bulk}.

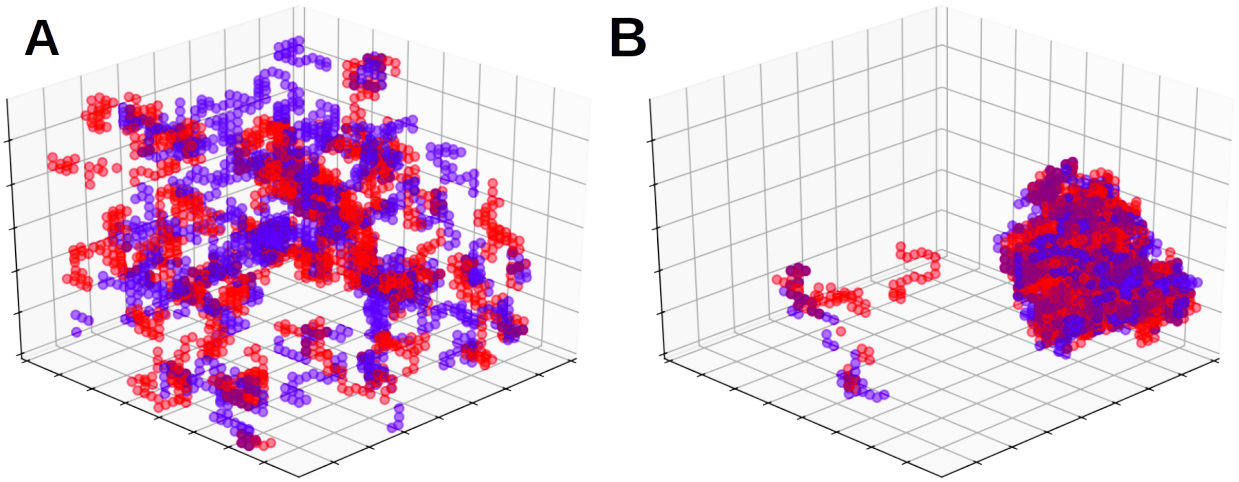

Figure S2: **Monte-Carlo Simulations of Bulk Lattice Polymers A**) Lattice polymer simulations show phase coexistence. Simulations at $0.25k_BT$ have a homogeneous polymer density.**B** Simulations at strong polymer coupling $1.0k_BT$, bottom, see coexisting dense and dilute phases.

2.3 Alternative bulk polymer mixtures

We also ran simulations with different bulk polymer mixtures and observed similar phases to those in our symmetric mix of red and blue polymers (See Figure S3). We simulated a unary polymer mixture with strong nearest-neighbor interactions, an asymmetric mixture of polymers (n=5 and n=20), and a mixture of two short (n=5) polymers. We observe one,two, and three surface phase-coexistence in all of these mixtures. The classical theories of wetting and prewetting only require a bulk systems that phase separates, and a surface with affinity for one of these phases. Diverse bulk systems ought display these phases, so long as they can phase-separate in the absence of a surface.

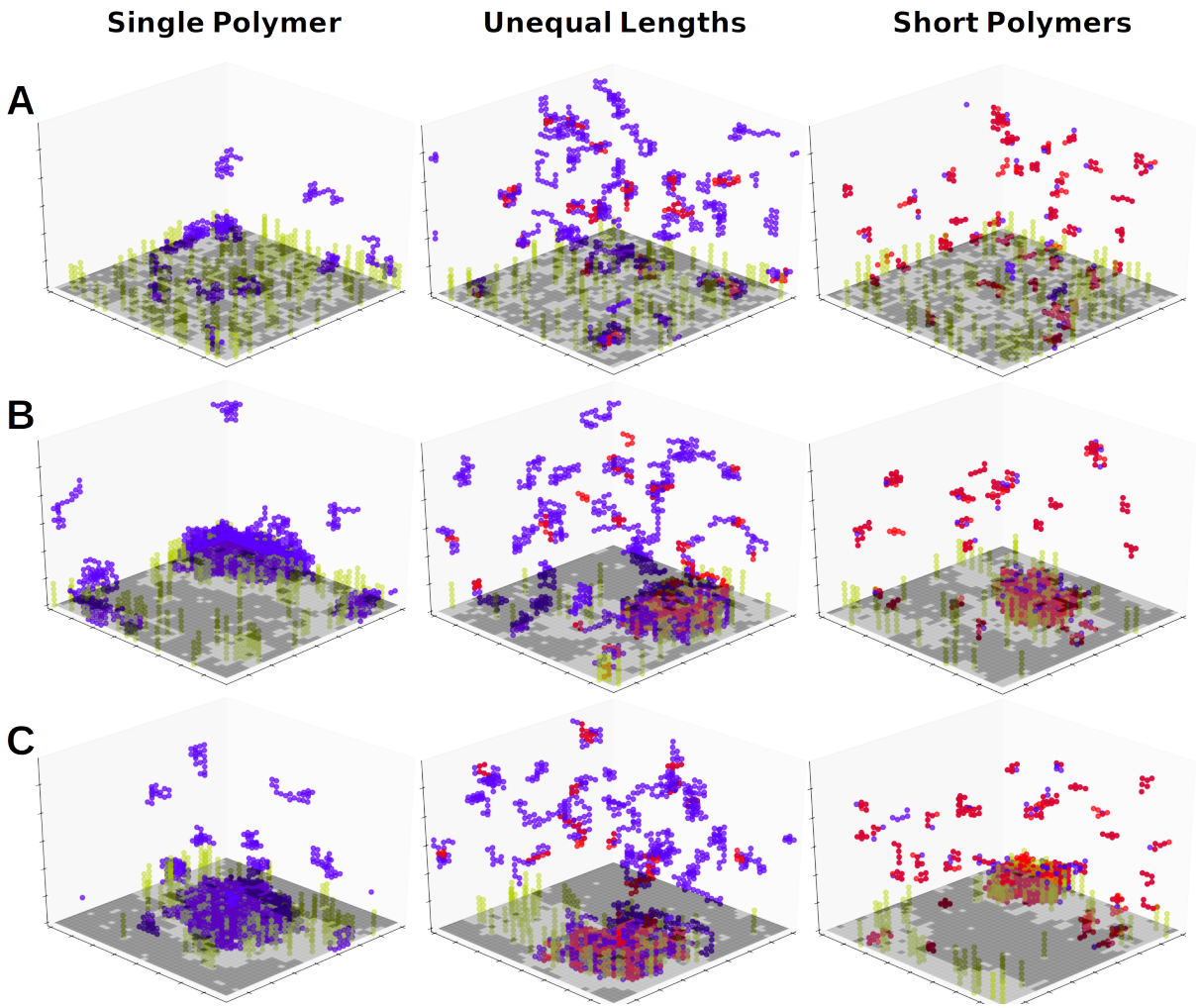

Figure S3: **Several Bulk Polymer Mixtures Produce Similar Results.** A) Single surface-phase system with a single polymer species (left), two polymers of unequal length (middle), and short polymers (right) B)Surface phase coexistence in mixtures as above C) Three surface phase coexistence

2.4 Two phase coexistence regions bound three-phase coexistence regions on the surface phase diagram

Our landau theory predicts three two-phase coexistence regions bounding the three-phase coexistence region (main text Figure 7A). We examined our Landau theory in these regions, Figure S4A. Shifting the surface composition eliminates one of the three stable solutions. After finding a parameter regime in simulations demonstrating three-phase coexistence we shifted membrane and tether compositions to access the two phase coexistence regions S4. Decreasing membrane order at constant tether density eliminates the prewet dry phase (l_d Dry-l_o Prewet). Likewise increasing membrane order with a slight increase in tether density shows l_o-Dry l_o-Prewet Coexistence. Finally, removing tethers eliminates the polymer rich phase, displaying a l_o-Dry l_d-Dry membrane.

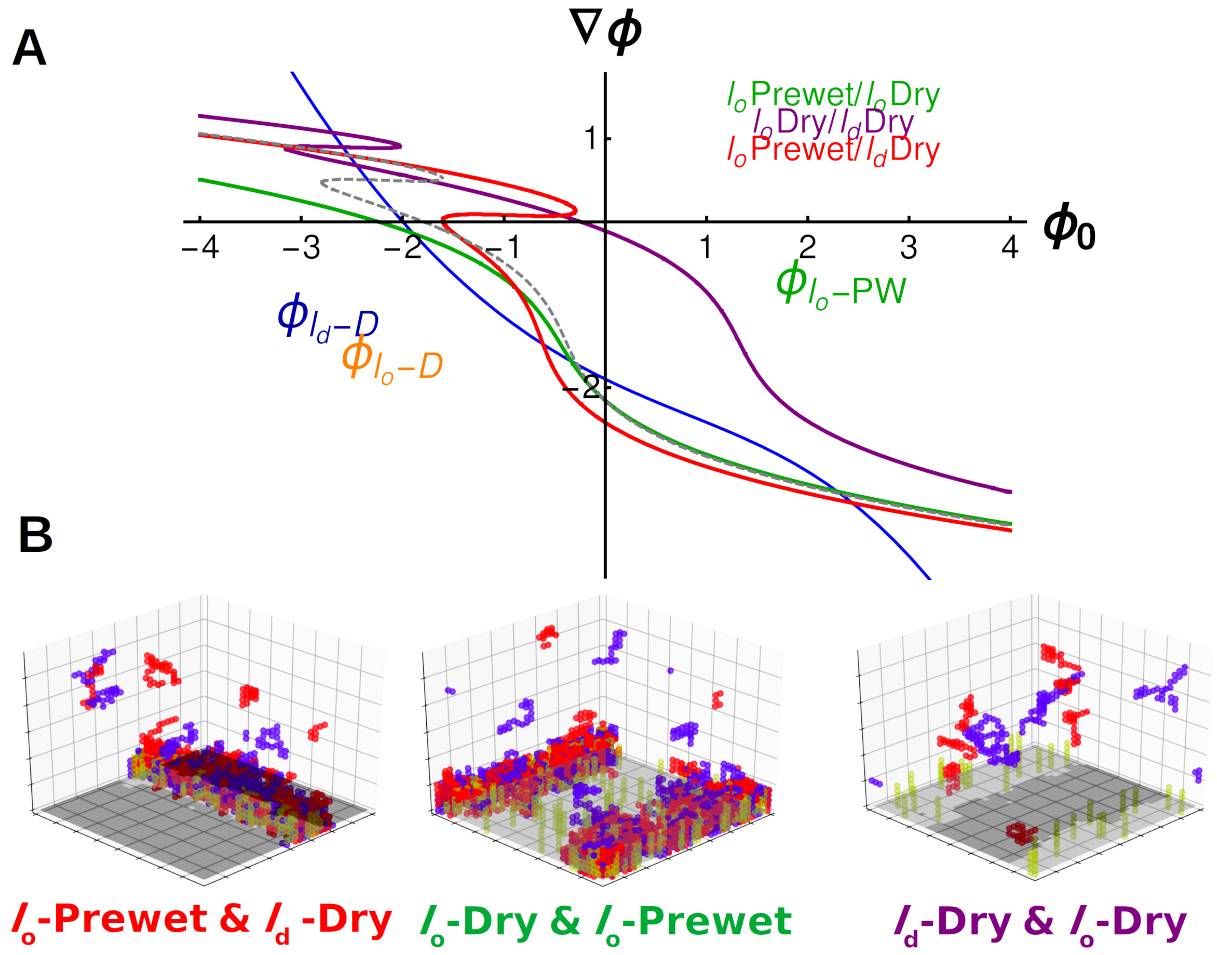

Figure S4: **Two-phase coexistence near three-phase coexistence A**) Gradient construction within each two phase region depicted in Figure 7A. **B**) Two-phase coexistence regions observed in simulation

2.5 Dependence of three-phase coexistence region on bulk and membrane temperatures

The three-phase coexistence region requires a phase-separated membrane and polymers that prewet in the absence of membrane interactions. We calculated the phase diagram in our Landau theory over membrane and bulk couplings in Figure S5A. Three-phase coexistence occurs at low membrane and bulk temperatures, and the parameter regime shrinks as either temperature is increased. We plotted the surface phase-diagram at several points within this phase diagrams in Figure S5B. Decreasing J_{mem} shrinks the l_o Dry -l_d-Dry coexistence region and respective edge of the three phase region. Decreasing J_{bulk} shrinks the l_o Dry-l_o Prewet coexistence region. Outside of the parameter regime where three-phases coexist, two-phases coexist. The character of these phases depends on whether the dominant force is membrane or bulk.

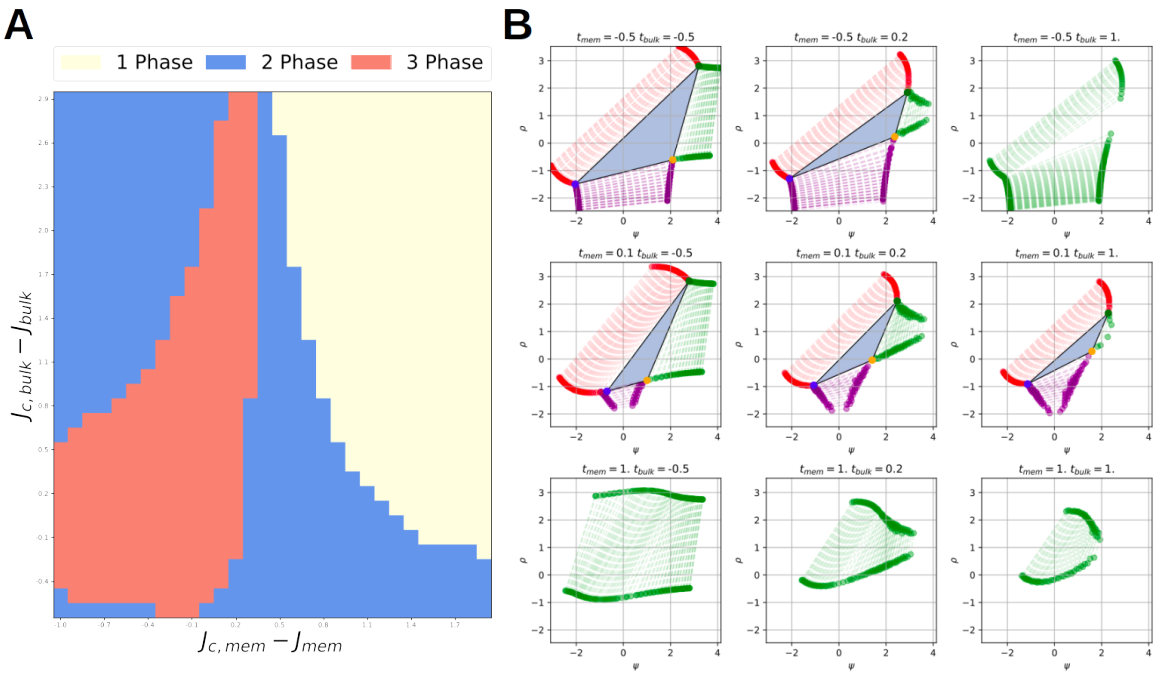

Figure S5: **Bulk and Membrane Coupling govern 3-phase coexistence A**) Phase diagram over membrane and bulk couplings showing one, two, and three phase regions (yellow, blue, and red). Three phase coexistence generally requires strong membrane and bulk interactions, but extends to weaker J_{bulk} near the membrane critical point. **B**) Surface phase diagrams at various membrane and bulk couplings. Weak membrane couplings collapse the purple (l_0-dry,l_d-dry) region, top to bottom. Weak bulk couplings shrink the green (l_o-prewet,l_o-dry) edge, left to right.

2.6 Surface densities may be dominated by bulk or membrane forces

Near $J_{c,mem}$, two surface phases coexist at very low J_{bulk}; at high J_{bulk} surface phases may also coexist at low J_{mem} (main text Figure 6A). We explored our Landau theory in these two limits to determine the character of these phases Figure S6. Order parameter profiles show that while the bulk-dominated phase is similar to that of classical prewetting [1] the membrane dominated phases only have marginal enrichment relative to the bulk equilibrium density ϕ_∞ as with a classical 'surface transition' [2]. This is similar to Nakanishi and Fisher's description of wetting and surface transitions [3], where surface transitions and prewetting are revealed to be the same transition viewed from different regions of a higher-dimensional phase diagram. Biological systems likely utilize these forces in a variety ways where membrane and bulk systems both have a role.

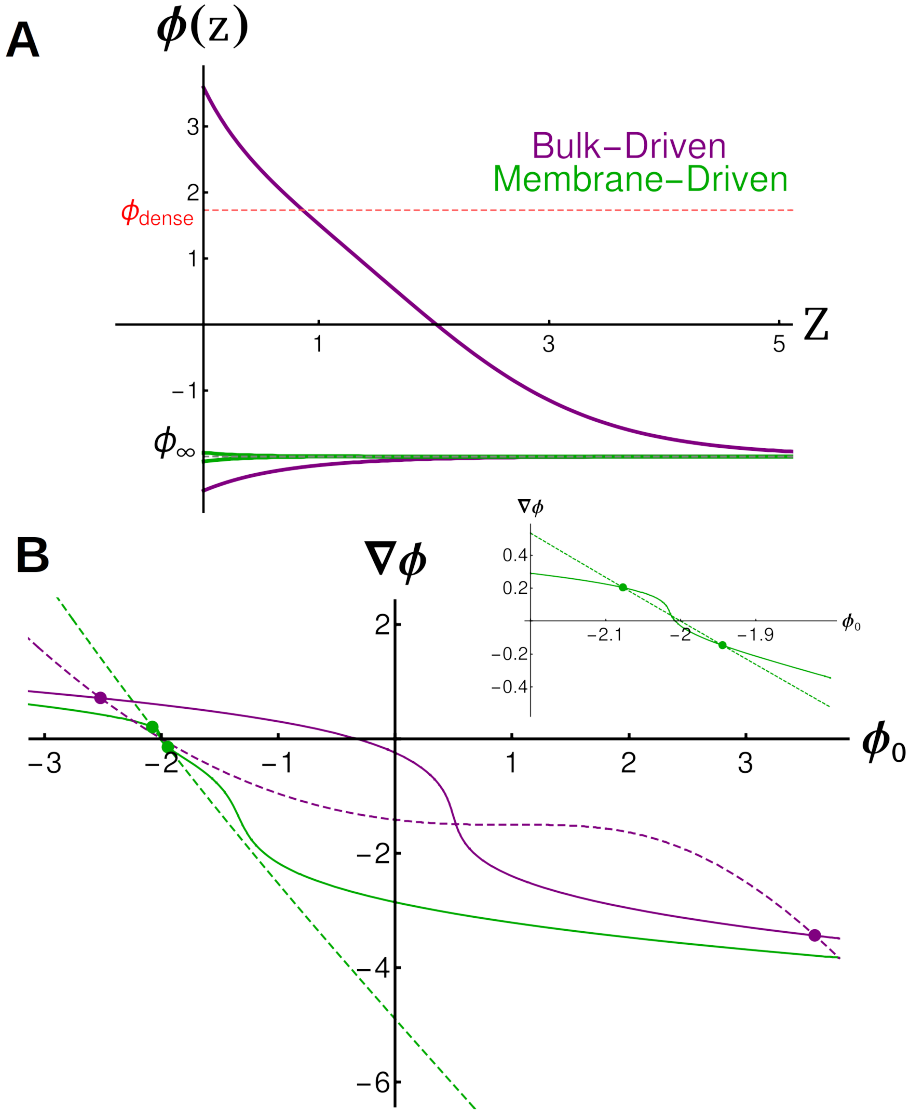

Figure S6: **Bulk and Membrane Dominated Surface densities A**) Density profiles for surface densities dominated by bulk (purple) and membrane (green) forces. **B**) Gradient construction for bulk and membrane dominated systems. A near-critical membrane allows surface coexistence when the gradient term is steep, but only over a narrow range of ϕ_0 values

2.7 Membrane composition and tether density alter surface polymer density

Our simulations show a strong dependence on membrane coupling and tether-bulk coupling. We explored the effect of surface composition, performing simulations varying tether density (see Figure S7A) and membrane composition (see Figure S7B) along with bulk coupling. We find that as tether density is increased, the density of polymers on the surface increases. As membrane order decreases towards the membrane critical point (membrane order = 0, or M =0), the density of surface polymers similarly increases. As membrane order further decreases, polymer density increases as tethers relegated to smaller regions on the membrane, effectively increasing their density

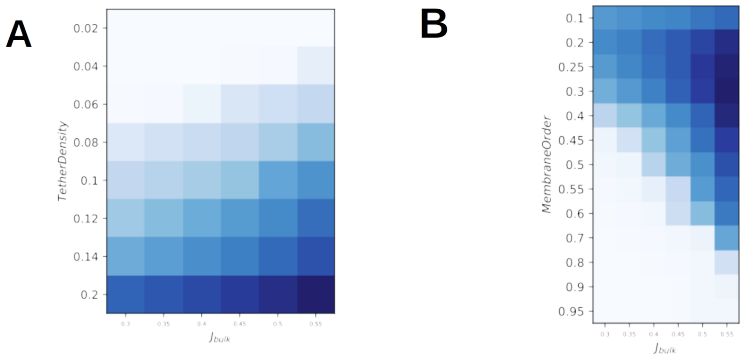

Figure S7: **Surface composition alters polymer density at the membrane**: **A**) Varying tether density and bulk coupling increases surface polymer density. High densities, dark blue; low densities, light blue. **B**) Decreasing membrane order increases surface polymer density

Table S1: Simulation parameters used in supplemental figures

Figure	**Tether Density**	**Membrane Order**	J_{bulk}, k_BT	J_{mem}, T_c	J_{tether}	μ_{bulk}
S1A/B	0.25	0.8	0.4	1.1	1.0	-4.5
S2A, One Phase	N/A	N/A	0.25	N/A	N/A	0.06
S2A, Coexistence	N/A	N/A	1.0	N/A	N/A	0.06
S3A Single	0.094	0.5	0.55	2.0	1.0	-4.5
S3A, Unequal	0.0625	0.5	1.62	2.0	1.0	-3.0
S3A, Short	0.0625	0.5	3.31	2.0	1.0	-3.5
S3B, Single	0.094	0.5	0.55	1.0	1.0	-4.5
S3B, Unequal	0.0625	0.5	1.62	1.0	1.0	-3.0
S3B, Short	0.0625	0.5	3.31	1.05	1.0	-3.5
S3C, Single	0.094	0.5	0.55	0.9	1.0	-4.5
S3C, Unequal	0.0625	0.5	1.64	0.0	1.0	-3.0
S3C, Short	0.0625	0.5	3.31	0.9	1.0	-3.5
S4B,$l_o - Prewet/l_d Dry$	0.08	0.2	0.5	0.5	1.0	-4.5
S4B, $l_o - Dry/l_o - Prewet$	0.14	1	0.5	0.5	1.0	-4.5
S4B, $l_d - Dry/l_o - Dry$	0.02	0.5	0.5	0.5	1.0	-4.5

References

[1] John W. Cahn. Critical point wetting. *The Journal of Chemical Physics*, 66(8):3667–3672, April 1977.

[2] R. Lipowsky. Surface-induced order and disorder: Critical phenomena at first-order phase transitions (invited). *Journal of Applied Physics*, 55(6):2485–2490, March 1984.

[3] Hisao Nakanishi and Michael E. Fisher. Multicriticality of Wetting, Prewetting, and Surface Transitions. *Physical Review Letters*, 49(21):1565–1568, November 1982.